Soft Matter

Determining the Elasto-adhesion Length by Void Collapse in Ultra-soft materials

Journal:	*Soft Matter*
Manuscript ID	SM-ART-10-2022-001333.R1
Article Type:	Paper
Date Submitted by the Author:	10-Dec-2022
Complete List of Authors:	Fu, Hongbo; University of Massachusetts Amherst, Polymer Science and Engineering Crosby, Alfred; University of Massachusetts, Polymer Science and Engineering

ARTICLE

Received 00th January 20xx,

Accepted 00th January 20xx

DOI: 10.1039/x0xx00000x

Determining the Elasto-adhesion Length by Void Collapse in Ultra-soft materials

Hongbo Fu,*[a] and Alfred J. Crosby [b]

The elasto-adhesion length (l_{EA}) is a materials property that describes the size scale where the relative importance of adhesion and elastic forces transitions for defined structures and functions. Conventional approaches for determining l_{EA} require independent measurements of the critical energy release rate (G_c) and Young's modulus (E). Herein, we introduce a new method to obtain l_{EA}, only relying upon visual inspection. This method relies upon the introduction of a controlled void within a soft material, for example an ultra-soft hydrogel as studied here. The geometry of the void within the hydrogel is tuned to control the relative strength of adhesion and elastic energy, and a relationship between the observed equilibrium configuration of the void and l_{EA} is derived. We validate this new method with independent force-based contact adhesion tests. This method allows for the easy measurement of l_{EA} for difficult-to-handle soft materials and can be amended for various chemistries and materials.

1. Introduction

The elasto-adhesion length, l_{EA}, is a material property that describes the influence of adhesion forces relative to elastic mechanical forces. The importance of this length scale has long been recognized in the design of adhesives[1–4], microelectromechanical systems (MEMS)[5–7], and microelectronic interconnects[8]; and its relevance is growing rapidly as soft materials engineering is expanding into a wide array of channels from robotics[9–11] to membranes[12,13]. In a formal sense, l_{EA} is the ratio of the adhesion energy per unit area, or the critical interfacial strain energy release rate (G_c), to the elastic modulus (E) of the material, or $l_{EA} = G_c/E$. This length scale represents a transitional border; whereby, performance capabilities, such as mold release, that occur on a size scale smaller than this length will be more influenced by adhesion rather than elastic properties, and conversely, those on larger size scales are more influenced by elasticity rather than interfacial adhesion properties. Hence, characterization of this size scale guides engineers in choosing proper materials or modifying their performance designs to accommodate anticipated limits.

Conventionally, materials engineers seek to measure G_c and E separately, subsequently calculating l_{EA} to guide designs. This direct approach can be tedious and time-consuming, especially for ultra-soft materials, where other challenges such as materials shaping, gripping, or gravitation-induced deformations, can complicate measurement procedures. Additionally, for many applications, the independent properties of G_c and E are not as important as the determination of l_{EA}, which dictates performance design. Here, we introduce a new method for measuring l_{EA}, which only relies upon visual inspection. We demonstrate this method for symmetric interfaces of ultra-soft hydrogel materials, but it is generally amenable to a wide range of chemistries and materials. We envision that this method offers pathways for high throughput materials characterization, especially for technologically driven materials development opportunities, due to its reliance only on visual inspection for quantitative materials property measurements.

The basic principle of acquiring the l_{EA} through visual inspection is to introduce a void with known dimensions and to observe the deformations induced by adhesion forces between opposing surfaces within the void. For such a cuboid void, as shown in Figure 1(b), with a rectangular shape and a controlled thickness, t, the void will be invisible when $l_{EA}/t >> 1$ and the adhesion energy dominates the deformation behavior, and the preset shape will persist when $l_{EA}/t << 1$, such that the elastic strain energy dominates. When $l_{EA}/t \sim 1$, the strain energy and adhesion energy balance to deform the initial defect shape into an equilibrium state with a shape intermediate to the two extremes. Hence, by observing the configuration with respect to the initial defect shape, l_{EA} can be determined.

We measure l_{EA} by observing the configuration of an initial cuboid void within a hydrogel material. This void is introduced by crosslinking the hydrogel around a thin, inert separator sheet in a cylindrical container and removing the sheet after the hydrogel network is formed (Figure 1(a)). The separator sheets

[a] *Address here.*
[b] *Address here.*
[c] *Address here.*
† Footnotes relating to the title and/or authors should appear here.
Electronic Supplementary Information (ESI) available: [details of any supplementary information available should be included here]. See DOI: 10.1039/x0xx00000x

have consistent width and height, and we vary the thickness to demonstrate the method. We observe the void shape and dimensions after removing the separator from the cured hydrogel. The system energy, including the strain and adhesion energy, is analyzed with the assistance of finite element analysis, and the relationship between l_{EA} and initial dimensions of the void within the hydrogel is determined. We refer to this method as the "Void Inspection Method," and we validate it with independent measurements of E and G_c of the same hydrogel composition using contact adhesion tests.

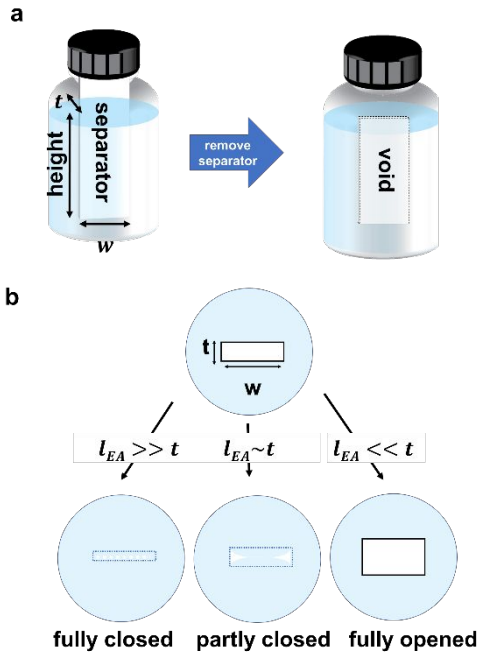

Figure 1. Void formation within hydrogels and the l_{EA} relationship with void geometries. (a) A schematic of preparing hydrogel cylinder with a cuboid void. (b) Anticipated hydrogel interface/surface behaviours with various thickness-l_{EA} ratios.

2. Experiments

2.1 Materials

Acrylamide, N,N'-methylenebis(acrylamide), ammonium persulfate (APS), and Tetramethylethylenediamine (TEMED) are purchased from Sigma-Aldrich and are used without processing. The Teflon® PTFE films and sheets with thickness ranging from 0.13mm to 3.08mm are purchased from McMaster-Carr and are cut into sheets with a consistent width of 15mm and length of 53mm.

2.2 Sample Preparation

The polyacrylamide (PAM) hydrogel with an internal cuboid void is prepared by inserting a PTFE sheet, which is referred to as the separator, in the precursor solution, as schematically shown in Figure 1(a). The separator is fixed to the vial cap and remains in the solution while the hydrogel is crosslinked. The separator is removed from the hydrogel after the crosslinking is complete, leaving a cuboid void within the hydrogel with initial dimensions of width (w) and thickness (t) set by the dimensions of the separator. The hydrogel precursor solution has a solid concentration of 5% and the ratio of the monomer to crosslinker is 100 to 1. Hydrogels are prepared in a glove bag to avoid oxygen contamination. We also prepare hydrogels with separators in ambient air atmosphere for a comparison study presented in section 3.5. We prepare hydrogel cylinders and spherical caps with the same composition under nitrogen atmosphere for the contact adhesion tests to compare the l_{EA} values. Detailed information of the steps for preparing the hydrogel spherical cap and cylinder for the contact adhesion tests is provided in the supplementary information in section S1.

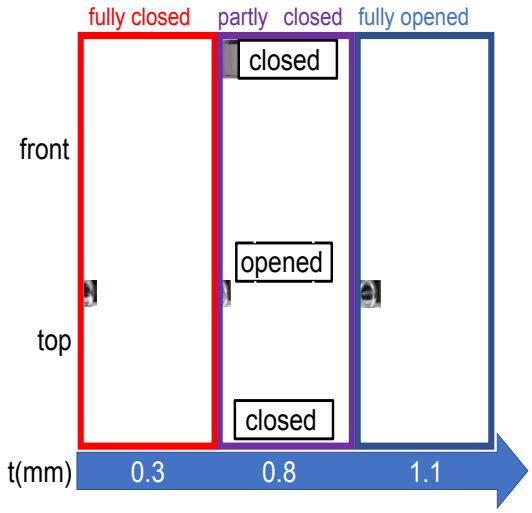

Figure 2. The close-to-open transition as the separator thickness increases.

3. Results and discussion

3.1 Hydrogel void surface/interface configurations

The effect of separator thickness on the hydrogel void configuration upon separator removal is investigated by varying the thickness with a fixed width and length. After removing the separator, the void surfaces of polyacrylamide hydrogel are exposed with a minimal distance determined by the separator thickness. Figure 2 shows three hydrogel interface/surface behaviors: (1) the two surfaces defined by the width of the cuboid void contact each other and form a nearly complete interface along the width if the separator thickness is below a critical value; (2) the interface between the two opposing surfaces only forms across a center region of the void with a width, w_c, at intermediate values of thickness; and (3) the surfaces remain open to form a cuboid void when the separator thickness is above a critical value. These regimes are defined by the competition between adhesion and elastic energy.

3.2 Surface/interface independence of kinetic history

To confirm that these regimes are energetically determined and not a result of kinetic history, we disrupt the as-formed interface in two different manners and confirm that the as-formed interface is achieved regardless of perturbation. First,

we mechanically open the initially closed interface by inserting a tweezer along the interface. The interface opens as the tweezer is inserted and returns to a closed state spontaneously once the tweezer is removed (Figure3(a)). Second, we mechanically force initially opened void surfaces to contact each other by applying compression force from the top. The surfaces contact and form an interface, but upon removal of the mechanical force the interface opens spontaneously (Figure3(b)).

To confirm the path-independence for the partially closed regime, we apply an impact load to the vial containing the hydrogel with the initially partially closed void. The closed width is normalized by the void width. The impact load is applied by tapping the vial on a rigid surface. Upon impact, the void closes completely, hence $w_c/w = 1$. Setting the time of impact as time equals zero, we then monitor the configuration of the void surfaces, w_c/w, as a function of time with the hydrogel vial at rest (Figure 3c). The interface formed between the hydrogel void surfaces separates, or fractures, from the two edges toward the center. This separation process stops at a final value of $w_c/w \approx 0.3$ to form the same partially closed void configuration that has been formed upon initial removal of the separator. Collectively, these experiments confirm that the configurations of the void surfaces after removing the separator are driven by the minimization of the total energy, and not path-dependent kinetics.

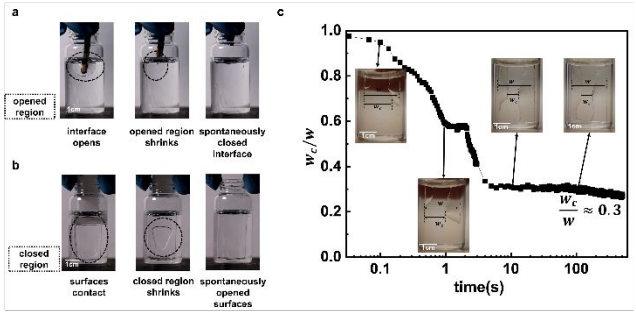

Figure 3. Perturbation independence of configurations. (a) A closed interface is forced open with a tweezer. After removing the external force, the interface recovers to a fully closed state. (b) Forcing an open interface to close through external compression with a plastic sheet. After releasing the external compressive force, the opened region propagates from the edge and drives the surface to the opened state. (c) The closed width, normalized by the total width, variation on time for a partly closed configuration. Insets: the configurations of the hydrogel at 0.1s, 1s, 10s, and 100s after stimuli, respectively. The region of measuring the closed width is marked. The video of the formation of the partly closed configuration is shown in supplementary video.

3.3 Total energy modeling

The total energy is the summation of the adhesion and strain energy contributions, expressed as:

$$\Pi_{tot} = \Pi_e + \Pi_a. \quad (1)$$

By relating each of these terms to the void geometry and the hydrogel materials properties, we develop a relationship between dimensions of the final void configuration and the elasto-adhesion length scale.

3.3.1 Adhesion energy

The expression of adhesion energy is straightforward. The adhesion energy is proportional to the exposed area when the fully closed configuration is regarded as the ground state:

$$\frac{\Pi_a}{E} = \frac{G_c}{E}(w - w_c) = l_{EA} w\left(1 - \left(\frac{w_c}{w}\right)\right). \quad (2)$$

Here we normalize the adhesion energy by Young's modulus in order to present the expression as a function of l_{EA}.

3.3.2 Elastic strain energy

The elastic strain energy is estimated from the work done by the attractive forces to deform the hydrogel void surfaces to form an interface:

$$\Pi_e = \int F d\delta \sim E\delta^2 \sim Et^2, \quad (3)$$

where F is the resultant force that displaces the void surface a distance of δ[14]. For a fully closed configuration, δ equates to t/2. Introducing K as a geometry-defined prefactor, the elastic strain energy is written as $\Pi_e/E = Kt^2$.

To determine the coefficient, finite element analysis is conducted. Considering the depth of the separator is larger than the thickness, we take the cross-section of the sample and analyze the strain energy per unit length with a 2-dimensional plane strain model, shown in Figure 4(a, inset), for a fixed ratio of void width, w, to vial diameter, D. We confirm that the strain energy is proportional to t^2. The geometrical coefficient K is determined from the linear fitting, shown in Figure 4(a). We note that this value of K is determined for a fixed ratio of $w/D = 0.3$, based upon our experimental conditions, and may vary for other geometric conditions.

For intermediate states where $0 < w_c/w < 1$, the strain energy is a function of w_c/w. We determine the strain energy from FEA simulations for configurations with different values of w_c/w and normalize by the strain energy for the fully closed state $w_c/w = 1$. The function $f\left(w_c/w\right)$ is found to be nonlinear, which we describe with a polynomial function:

$$f\left(\frac{w_c}{w}\right) = \sum_{i=1}^{4} m_i \left(\frac{w_c}{w}\right)^{i-1}. \quad (4)$$

where m_i is a series of unitless factors (Figure 4(b)). The details of the FEA simulation and the determination of $f(w_c/w)$ are provided in SI section S3. The determined unitess prefactors, {m1, m2, m3, m4}, are {1.3948, -0.9290, 0.5337, 0.0011}, respectively. Based on this approach, the elastic strain energy per unit length can be expressed as:

$$\frac{\Pi_e}{E} = Kt^2 f\left(\frac{w_c}{w}\right). \quad (5)$$

3.3.3 Expression of l_{EA}

Summing equations (2) and (5), we determine an expression for the total energy as a function of w_c/w. The equilibrium configuration is determined when the total energy is minimized with respect to w_c/w, and from this condition we determine a relationship between the elasto-adhesion length and w_c/w for given values of t and w:

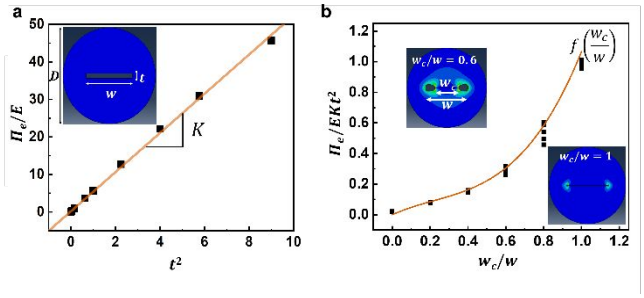

Figure 4 Strain energy analysis from FEA (a) The strain energy variation as a function of separator thickness when $w_c/w = 1$. Inset: geometrical factors of the 2-D model. Error bars are not shown since mesh variation studies were not conducted. Details on the mesh generation and element type for the FEA are provided in section S3 in the supplementary information. (b) The strain energy dependence on closed width, normalized by the strain energy at the fully closed ($w_c/w = 1$) state. For each value of w_c/w, we determined the strain energy at five different values of t: 0.8, 1.0, 1.5, 2.0 and 2.4. inset: the deformed configuration at $w_c/w = 0.6$, and $w_c/w = 1$ from the FEA model. $w/D = 0.3$ is fixed among FEA simulations to keep consistent with the experimetnal geometry. The detailed information of FEA is introduced in section S3 in the supplementary information.

$$l_{EA} = \frac{Kt^2 f'\left(\frac{w_c}{w}\right)}{w}. \quad (6)$$

Here f' is the first derivative of f.

3.4 Example and Validation

As an example, we can determine l_{EA} from the experimental result provided in Figure 2(c). The normalized equilibrium closed width is $w_c/w = 0.29$; the initial width of cuboid is $w = 15mm$; and the thickness of the cuboid is $t = 0.79mm$. Thus, for this polyacrylamide hydrogel sample, the elasto-adhesion length is $l_{EA} = 0.089mm$. We made these measurements for four replicate samples, with the same components of the hydrogel and the same dimensions of the separator, to demonstrate the reproducibility of this method.

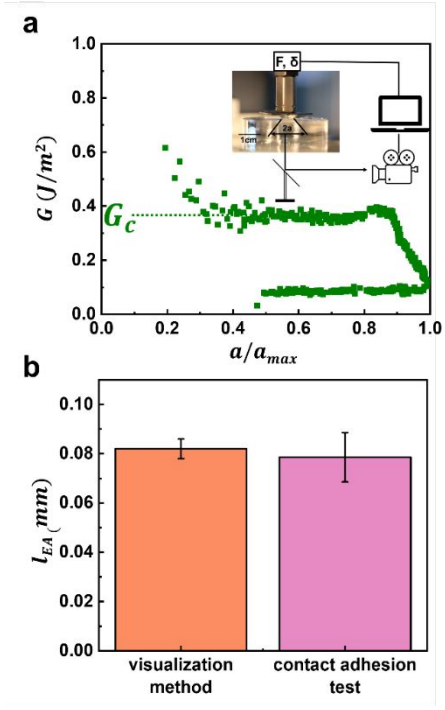

Figure 5 The elasto-adhesion length analysis (a) The energy release rate versus the normalized contact radius for hydrogel interfaces cured in nitrogen. The plateau regime is marked as G_c. Inset: schematic of a force-based contact adhesion test. (b) The cross-platform comparison of l_{EA}. The error bar of void collapse inspection method is from the standard deviation of four replicates. The error bar of the contact adhesion test is one standard deviation of the averaged energy release rate.

From these measurements, the mean elasto-adhesion length is $l_{EA} = 0.082 \pm 0.004mm$, as shown in the supplementary information in section S4.

To validate the void collapse inspection method, we conduct a force-based contact adhesion test, as shown in Figure 5(a, inset), to determine G_c and E, hence l_{EA}. In these experiments, a polyacrylamide hydrogel shaped as a spherical cap with a radius of curvature, $R = 8.0mm$, is brought into contact with and then separated from the flat end of polyacrylamide hydrogel cylinder. The relative displacement between the two polyacrylamide hydrogels is controlled at a fixed displacement rate of 0.01mm/s while the resulting force and contact area are recorded. From the resulting force and contact area, we calculate G as a function of contact radius, a, using the equations and procedure described in the supplementary information[15–20] in section S5. During interface formation, or loading, G is in the range of 10^{-2}J/m^2. As the interface is separated, G increases and reaches a plateau, valued as $G_c = 0.35J/m^2$, during which the contact radius decreases until detachment, shown in Figure 5(a).

For the contact adhesion tests, the two hydrogel contacting surfaces are cured under slightly different conditions necessitated by the need to achieve different geometric shapes. The hydrogel cylinder is cured in nitrogen atmosphere such that the flat end surface is in contact with a PTFE sheet during curing to replicate the curing condition for the hydrogel surface used in the void inspection method. The hydrogel spherical cap is cured under a nitrogen atmosphere, but its surface is only exposed to the atmosphere and not in contact with PTFE. Therefore, to calculate l_{EA} from the contact adhesion test, we measured Young's moduli of the cylindrical hydrogel and the spherical cap separately using indentation methods. The modulus of the cylindrical hydrogel is measured with a flat steel probe indentation test, such that the contact area is fixed[15,19,21,22]. The modulus of the spherical hydrogel probe is measured by contacting it with a glass slide, and the contact area and resulting force are measured as a function of the relative displacement[19]. The Young's modulus of the cylindrical hydrogel is $E_{cy} = 4.12kPa$ while Young's modulus of the spherical cap is $E_{sph} = 5.38kPa$. We use the harmonic mean of the moduli as the system average modulus, $E_{avg} = 4.67kPa$, [15]and calculate the elasto-adhesion length from the contact adhesion tests to be $l_{EA,CAT} = 0.078 \pm 0.010mm$. The algorithms used in determining Young's moduli of the hydrogel cylinders and spheres are provided in section S2 in the supplementary information. The p-value of the two methods shows that the difference between the two methods is insignificant, as shown in section S6 of the supplementary information. As the elasto-adhesion length values from two independent methods are within error of each other (Figure 5(b)), the void collapse inspection method is validated.

3.5 Sensitivity of the void collapse inspection method to hydrogel curing condition

To demonstrate the sensitivity of the void collapse method, we measure the differences in the elasto-adhesion length scale for polyacrylamide hydrogels cured in different environments. It is well-known that oxygen in the air can diffuse into polyacrylamide precursor solutions and inhibit the propagation of polymer chains and enhance the formation of dangling ends in the polymer network[23,24]. Such chain defects in the polymer network can cause fewer effective crosslinks, thus reducing the elastic modulus[25–27]. We prepare two series of hydrogel samples with the same composition and the same separator geometry. One series is cured in the air, and the other series is cured in a nitrogen environment. Comparing the two series of hydrogels,

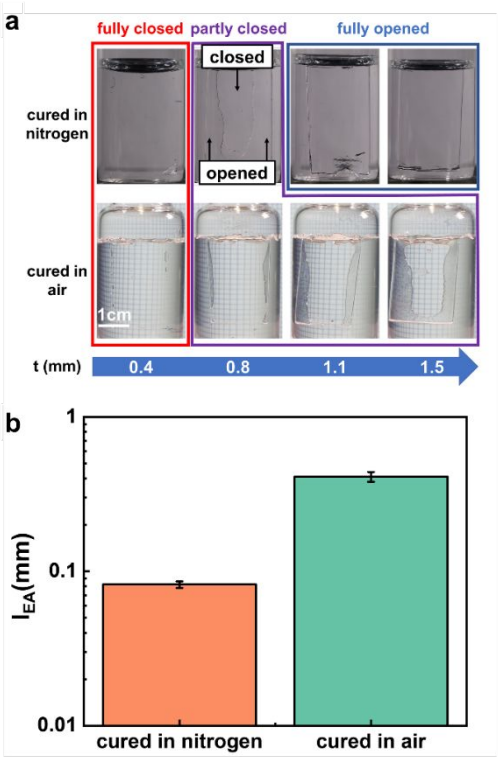

Figure 6 Application of the void collapse inspection method in PAM hydrogels cured in air. (a) The comparison of surface configurations for the hydrogel cured in nitrogen versus cured in air at the same separator thicknesses. (b) The l_{EA} comparison of PAM hydrogels with different curing environments, in nitrogen versus in air. The error bar of "cured in air" hydrogels is from the standard error of the linear fitting, shown in Figure (s5).

the corresponding separator thicknesses for the partly closed configuration are different (Figure 6(a)), indicating a different l_{EA} for the networks cured in air compared to those cured under nitrogen synthesized with the identical precursor solution. Based on Equation 6, $l_{EA} = 0.41mm$ for the cured in air material, as compared to 0.089mm for the cured in nitrogen network. The l_{EA} of cured in air hydrogel is approximately four times larger compared with the hydrogels cured in nitrogen atmosphere (Figure 6(b)). To the best of our knowledge, a similar measurement is difficult to replicate with any other adhesion measurement. For such a small hydrogel sample as a spherical cap, oxygen diffuses into the solution thoroughly during curing and thus no solid will be formed. The void collapse inspection method is convenient for overcoming difficulties of preparing soft hydrogels specimens and controlling consistent conditions of sample preparation.

Conclusions

In conclusion, we have demonstrated that systematically defined voids, such as the cuboids introduced here, can provide a simple visual measurement of the elasto-adhesion length scale. The competition between elastic energy and surface energy determines the final equilibrium configuration of the void: fully closed, partly closed, or fully opened. From the partly closed configurations, l_{EA} is determined by the dimensions of the closed interfacial width. We validated this method with independently measured values of l_{EA} and demonstrated its sensitivity by measuring l_{EA} for polyacrylamide hydrogels cured under different atmospheres. Overall, this method provides a straightforward determination of l_{EA} using visual inspection alone, thus opening pathways for high-throughput measurements and formulation development. Future studies on hydrogels and other soft materials with a larger range of moduli and adhesion energies, including materials with dynamic or asymmetric interfaces, which will provide rich insight into the benefits of this method and how it can directly influence interfacial engineering.

Author Contributions

Hongbo Fu, as the first author, is responsible for conceptualization, data acquisition, formal analysis, and original draft writing. Alfred Crosby, as the corresponding author, is responsible for validation, supervision, and review editing.

Conflicts of interest

There are no conflicts to declare.

Acknowledgments

The authors acknowledge the support from the Office of Naval Research Grant (ONR N00014-17-1- 2056).

Notes and references

1 C.-Y. Hui, J. A., S. J. Bennison and J. D. Londono, *Proc. R. Soc. London. Ser. A Math. Phys. Eng. Sci.*, 2003, **459**, 1489–1516.
2 R. Villey, C. Creton, P. P. Cortet, M. J. Dalbe, T. Jet, B. Saintyves, S. Santucci, L. Vanel, D. J. Yarusso and M. Ciccotti, *Soft Matter*, 2015, **11**, 3480–3491.
3 C. Creton and M. Ciccotti, *Reports Prog. Phys.*, 2016, **79**, 046601.
4 T. J. S. Wilting, M. H. Essink, H. Gelderblom and J. H. Snoeijer, *Europhys. Lett.*, 2021, **134**, 56001.
5 C. A. Morrow and M. R. Lovell, *J. Tribol.*, 2005, **127**, 447–450.
6 J.-L. Liu and R. Xia, *Acta Mech. Sin.*, 2013, **29**, 62–72.

7 R. W. Style, A. Jagota, C.-Y. Hui and E. R. Dufresne, *Annu. Rev. Condens. Matter Phys.*, 2017, **8**, 99–118.
8 G. Raos and B. Zappone, *Macromolecules*, 2021, 54, 10617–10644.
9 J. Liu, S. Qu, Z. Suo and W. Yang, *Natl. Sci. Rev.*, 2021, **8**, 2021.
10 R. Long, C.-Y. Hui, J. P. Gong and E. Bouchbinder, *Annu. Rev. Condens. Matter Phys.*, 2021, **12**, 71–94.
11 N. Kazem, M. D. Bartlett and C. Majidi, *Adv. Mater.*, 2018, **30**, 1706594.
12 A. Z. Dookhith, N. A. Lynd, C. Creton and G. E. Sanoja, *Macromolecules*, 2022, **55**, 5601–5609.
13 A. Chakrabarti and M. K. Chaudhury, *Langmuir*, 2013, **29**, 15543–15550.
14 A. Flamant, *CR Acad. Sci. Paris*, 1892, **114**, 1465–1468.
15 K. L. Johnson, K. Kendall and A. D. Roberts, *Proc. R. Soc. A Math. Phys. Eng. Sci.*, 1971, **324**, 301–313.
16 D. Maugis and M. Barquins, *J. Phys. D. Appl. Phys.*, 1978, **11**, 1989–2023.
17 D. Maugis and M. Barquins, in *Adhesion and Adsorption of Polymers*, Springer US, Boston, MA, 1980, vol. 12 A, pp. 203–277.
18 D. Maugis, *J. Adhes. Sci. Technol.*, 1987, **1**, 105–134.
19 K. R. Shull, D. Ahn, W. L. Chen, C. M. Flanigan and A. J. Crosby, *Macromol. Chem. Phys.*, 1998, **199**, 489–511.
20 A. J. Crosby and K. R. Shull, *J. Polym. Sci. Part B Polym. Phys.*, 1999, **37**, 3455–3472.
21 S. Rattan, L. Li, H. K. Lau, A. J. Crosby and K. L. Kiick, *Soft Matter*, 2018, **14**, 3478–3489.
22 H. K. Lau, S. Rattan, H. Fu, C. G. Garcia, D. M. Barber, K. L. Kiick and A. J. Crosby, *Macromol. Biosci.*, 2020, **20**, 1900360.
23 C. J. Yeh, M. Hu and K. R. Shull, *Macromolecules*, 2018, **51**, 5511–5518.
24 N. G. Gaylord and C. Walling, *J. Polym. Sci.*, 1959, **35**, 317–318.
25 M. Zhong, R. Wang, K. Kawamoto, B. D. Olsen and J. A. Johnson, *Science (80-.).*, 2016, **353**, 1264–1268.
26 E. Ducrot, Y. Chen, M. Bulters, R. P. Sijbesma and C. Creton, *Science (80-.).*, 2014, **344**, 186–189.
27 P. J. Flory, *Br. Polym. J.*, 1985, **17**, 96–102.